eNeuro

Research Article: New Research | Disorders of the Nervous System

Atypical Localization and Dissociation between Glucose Uptake and Amyloid Deposition in Cognitively-Normal APOE*E4 Homozygotic Elders Compared to Patients with Late-Onset Alzheimer's Disease

José V. Pardo[1,2], Joel T. Lee[1,2] and for Alzheimer's Disease Neuroimaging Initiative

[1]*Cognitive Neuroimaging Unit, Mental Health Service Line, Minneapolis Veterans Health Care System, Minneapolis, MN 55417, USA*

[2]*Department of Psychiatry, University of Minnesota, Minneapolis, MN 55455, USA*

DOI: 10.1523/ENEURO.0396-17.2018

Received: 23 October 2017

Revised: 22 January 2018

Accepted: 6 February 2018

Published: 15 February 2018

Author Contributions: Each author must be identified with at least one of the following: Designed research, JVP and JTL designed the research, analyzed data, contributed analytic tools, and wrote the paper. ADNI provided data as indicated in acknowledgments.

Funding: http://doi.org/10.13039/100000738U.S. Department of Veterans Affairs (VA)
VA 5I01CX000501

Conflict of Interest: Authors report no conflict of interest.

This work was funded by VA 5I01CX000501 (JVP). This material is the result of work supported with resources and the use of facilities at the Minneapolis Veterans Health Care System, Minneapolis, MN. The contents do not represent the views of the U.S. Department of Veterans Affairs or the United States Government.

Data used in preparation of this article were obtained from the Alzheimer's Disease Neuroimaging Initiative (ADNI) database (adni.loni.usc.edu). As such, the investigators within the ADNI contributed to the design and implementation of ADNI and/or provided data but did not participate in analysis or writing of this report. A complete listing of ADNI investigators can be found at http://adni.loni.usc.edu/wp-content/uploads/how_to_apply/ADNI_Acknowledgement_List.pdf

Data collection and sharing for this project was funded by the Alzheimer's Disease Neuroimaging Initiative (ADNI) (National Institutes of Health Grant U01 AG024904) and DOD ADNI (Department of Defense award number W81XWH-12-2-0012). ADNI is funded by the National Institute on Aging, the National Institute of Biomedical Imaging and Bioengineering, and through generous contributions from the following: AbbVie, Alzheimer's Association; Alzheimer's Drug Discovery Foundation; Araclon Biotech; BioClinica, Inc.; Biogen; Bristol-Myers Squibb Company; CereSpir, Inc.; Cogstate; Eisai Inc.; Elan Pharmaceuticals, Inc.; Eli Lilly and Company; EuroImmun; F. Hoffmann-La Roche Ltd and its affiliated company Genentech, Inc.; Fujirebio; GE Healthcare; IXICO Ltd.; Janssen Alzheimer Immunotherapy Research & Development, LLC.; Johnson & Johnson Pharmaceutical Research & Development LLC.; Lumosity; Lundbeck; Merck & Co., Inc.; Meso Scale Diagnostics, LLC.; NeuroRx Research; Neurotrack Technologies; Novartis Pharmaceuticals Corporation; Pfizer Inc.; Piramal Imaging; Servier; Takeda Pharmaceutical Company; and Transition Therapeutics. The Canadian Institutes of Health Research is providing funds to support ADNI clinical sites in Canada. Private sector contributions are facilitated by the Foundation for the National Institutes of Health (www.fnih.org). The grantee organization is the Northern California Institute for Research and Education, and the study is coordinated by the Alzheimer's Therapeutic Research Institute at the University of Southern California. ADNI data are disseminated by the Laboratory for Neuro Imaging at the University of Southern California.

Correspondence should be addressed to José V. Pardo, MD, PhD, Minneapolis VA Medical Center, One Veterans Drive, Minneapolis, MN 55417, USA. E-mail: jvpardo@umn.edu

Cite as: eNeuro 2018; 10.1523/ENEURO.0396-17.2018

1. Manuscript Title (50 word maximum)

Atypical localization and dissociation between glucose uptake and amyloid deposition in cognitively-normal APOE*E4 homozygotic elders compared to patients with late-onset Alzheimer's disease

2. Abbreviated Title (50 character maximum)

FDG and amyloid PET in healthy APOE*E4 elderly homozygotes

3. List all Author Names and Affiliations in order as they would appear in the published article

José V. Pardo[1,2] & Joel T. Lee[1,2] for the Alzheimer's Disease Neuroimaging Initiative*

[1] Cognitive Neuroimaging Unit, Mental Health Service Line, Minneapolis Veterans Health Care System, Minneapolis, MN 55417

[2]Department of Psychiatry, University of Minnesota, Minneapolis, MN 55455

4. Author Contributions: Each author must be identified with at least one of the following: Designed research,

JVP and JTL designed the research, analyzed data, contributed analytic tools, and wrote the paper. ADNI provided data as indicated in acknowledgments.

5. Correspondence should be addressed to (include email address)

José V. Pardo, M.D., Ph.D.; Minneapolis VA Medical Center; One Veterans Drive; Minneapolis, MN; 55417; jvpardo@umn.edu

6. Number of Figures 2
7. Number of Tables 2
8. Number of Multimedia 0

9. Number of words for Abstract 230
10. Number of words for Significance Statement 115
11. Number of words for Introduction 730
12. Number of words for Discussion 3000

13. Acknowledgements

*Data used in preparation of this article were obtained from the Alzheimer's Disease Neuroimaging Initiative (ADNI) database (adni.loni.usc.edu). As such, the investigators within the ADNI contributed to the design and implementation of ADNI and/or provided data but did not participate in analysis or writing of this report. A complete listing of ADNI investigators can be found at http://adni.loni.usc.edu/wp-content/uploads/how_to_apply/ADNI_Acknowledgement_List.pdf

Data collection and sharing for this project was funded by the Alzheimer's Disease Neuroimaging Initiative (ADNI) (National Institutes of Health Grant U01 AG024904) and DOD ADNI (Department of Defense award number W81XWH-12-2-0012). ADNI is funded by the National Institute on Aging, the National Institute of Biomedical Imaging and Bioengineering, and through generous contributions from the following: AbbVie, Alzheimer's Association; Alzheimer's Drug Discovery Foundation; Araclon Biotech; BioClinica, Inc.; Biogen; Bristol-Myers Squibb Company; CereSpir, Inc.; Cogstate; Eisai Inc.; Elan Pharmaceuticals, Inc.; Eli Lilly and Company; EuroImmun; F. Hoffmann-La Roche Ltd and its affiliated company Genentech, Inc.; Fujirebio; GE Healthcare; IXICO Ltd.; Janssen Alzheimer Immunotherapy Research & Development, LLC.; Johnson & Johnson Pharmaceutical Research & Development LLC.; Lumosity; Lundbeck; Merck & Co., Inc.; Meso Scale Diagnostics, LLC.; NeuroRx Research; Neurotrack Technologies; Novartis Pharmaceuticals Corporation; Pfizer Inc.; Piramal Imaging; Servier; Takeda Pharmaceutical Company; and Transition Therapeutics. The Canadian Institutes of Health Research is providing funds to support ADNI clinical sites in Canada. Private sector contributions are facilitated by the Foundation for the National Institutes of Health (www.fnih.org). The grantee organization is the Northern California Institute for Research and Education, and the study is coordinated by the Alzheimer's Therapeutic Research Institute at the University of Southern California. ADNI data are disseminated by the Laboratory for Neuro Imaging at the University of Southern California.

14. Conflict of Interest

Authors report no conflict of interest.

Funding sources

This work was funded by VA 5I01CX000501 (JVP). This material is the result of work supported with resources and the use of facilities at the Minneapolis Veterans Health Care System, Minneapolis, MN. The contents do not represent the views of the U.S. Department of Veterans Affairs or the United States Government.

Abstract

Alzheimer's disease (AD) progresses insidiously over decades. Therefore, study of preclinical AD is critical to identify early pathophysiological changes as potential targets for prevention or treatment. The brain processes at the preclinical stage remain minimally understood. Aside from age, the E4 allele of APOE flags a group at particularly high risk of late onset AD (LOAD). Studies of these individuals could provide insights about the ontogenesis of AD offering clues for novel treatment strategies. To this end, cognitively-normal, *APOE*E4* homozygotes from the Alzheimer's Diseases Neuroimaging Research Initiative database (ADNI-LONI) provided fluorodeoxyglucose and amyloid (florbetapir) PET scans (N = 8 and 7, respectively; mean age 76 years). Their scans were compared to those of matched cognitively-normal elders who were not E4 carriers. There was dissociation in the distribution between glucose uptake and amyloid deposition in the homozygotes. Peak hypometabolism localized bilaterally along the medial temporal cortex. In contrast, peak amyloid deposition localized principally to the putamen--a finding also seen in preclinical carriers of autosomal dominant AD mutations and preclinical AD associated with Down's syndrome. Additional regions of amyloid deposition in homozygotes were medial prefrontal cortices including the anterior cingulate, middle and inferior frontal cortices, and middle and inferior occipital cortices. These findings contrast with those reported for LOAD. These data begin to characterize elders with normal cognition despite high AD risk in comparison to the known phenotypes of patients with LOAD.

Significance Statement

*APOE*E4* has the largest single effect size of any common variant for any human disease. *APOE*E4* homozygotes increase the risk of late onset Alzheimer's disease (LOAD) fifteen-fold. Research indicates interventions for AD must occur decades before onset of symptoms. However, the phenotypic antecedents and pathophysiology of LOAD remain limited in characterization. *APOE*E4* homozygotes offer a unique opportunity to characterize preclinical AD. Here, neuroimaging of cognitively-normal, elderly *APOE*E4* homozygotes reveals decreased medial temporal metabolism and increased lenticular amyloid deposition in those at high risk for developing LOAD. In comparison to LOAD, an atypical pattern of change in metabolism and amyloid distribution as well as a dissociation between these two measures arose in homozygotes compared to non-carriers.

Introduction

Alzheimer's disease (AD) disease process begins insidiously decades before enough brain damage occurs to require accessing medical care. Increasingly, there is consensus that prevention is critical and that interventions will be best when used early. The two most significant risk factors for AD are age and the *APOE*E4* gene (also referred to as E4).

Having two *APOE*E4* alleles gives an odds-ratio for AD of almost fifteen (Farrer et al., 1997). *APOE*E4* is the common variant with the greatest known effect size for association to any human disease. This level of risk is like that for known Mendelian disease-causing mutations such as the breast cancer gene, *BRACA* (Genin et al., 2011). E4 homozygotes have earlier onset of cognitive decline by approximately 5-7 years (Blacker et al., 1997; Sando et al., 2008). Therefore, studies of carriers of *APOE*E4* have the potential to reveal insights into the early pathophysiology of AD. Recent advances in technology offer unique opportunities to study these individuals non-invasively.

Early in the development of AD, amorphous amyloid deposits occur throughout the brain initially in the inferior aspects of the frontal, temporal, and occipital lobes, later spreading diffusely throughout the neocortex (Braak & Braak, 1991). Amyloid deposition in the form of neuritic plaques containing the amyloid-beta (Aß) protein develop with variable consistency, density, and distribution. Tangles and neuropil threads generally develop before plaques. The presence of *APOE*E4* is associated with amyloid deposition even in cognitively normal elders (Morris et al., 2010). The amount and

distribution of neuritic plaques vary widely between individuals at similar disease stages (Braak and Braak, 1991). As many as one-third of E4 non-carriers diagnosed clinically with AD are characterized as amyloid negative on neuropathologic assessment (Monsell et al., 2015). In that study, approximately one-half of those with a primary diagnosis of mild to moderate AD and low cerebral Aß had extensive neurofibrillary degeneration.

The amount of fibrillar amyloid throughout the brain both identifies past and future decline in cognition (Doraiswamy et al., 2014; Donohue et al., 2017). PET studies of AD indicate fibrillar amyloid and hypometabolism arise early in the posterior cingulate cortex/precuneus (Minoshima et al., 1994; Minoshima et al., 1997; Scheff et al., 2015). Although there is often overlap between cortical thinning, amyloid deposition, and hypometabolism, dissociations are not unusual (Murray et al., 2014).

Abnormal tau begins to deposit in the transentorrhinal cortex even in non-demented individuals (Braak and Braak, 1991; Bouras et al., 1994; Braak and Del Tredici, 2015). Subsequently, tau spreads to limbic allocortices including the hippocampal, cingulate, retrosplenial, and orbitofrontal cortices. With advanced AD, tau spreads into the neocortex. Tau staging correlates best with the level of cognitive function and appears consistent across individuals with similar symptoms and degrees of clinical dysfunction (Braak and Braak, 1991; Ossenkoppele et al., 2016). *APOE*E4* status and tau pathology are not correlated (Morris et al., 2010). Although there is frequent overlap between amyloid, atrophy, and tau, dissociation between markers can occur; tau and atrophy tend to co-occur more frequently (Xia et al., 2017).

Biomarker development has advanced greatly the characterization of preclinical and early AD. As many as 30% of cognitively-normal individuals over 65 years of age have significant amyloid deposition (Murray et al., 2014). PET imaging has demonstrated amyloid deposition in both cognitively intact as well as impaired carriers of mutations in PSEN1, PSEN2, and APP, who typically have early onset of AD (Klunk et al., 2007; Remes et al., 2008; Fleisher et al., 2012; Shi et al., 2015; Rodriguez-Vieitez et al., 2016). Similarly, amyloid deposition has been found in those with and without evidence of cognitive decline who have Down's syndrome (trisomy 21) with development of AD during middle age (Handen et al., 2012; Lao et al., 2016; Rafii et al., 2017).

Cognitively-normal healthy elders homozygous for *APOE*E4* and therefore at very high risk of developing AD, could provide data relevant to preclinical AD. Such information can guide future research and hint at pathophysiological mechanisms, particularly given recent evidence from transgenic mice that *APOE*E4* may provide a gain-of-toxic function independently of amyloid (Shi et al., 2017). To this end, PET scans of glucose uptake with ^{18}F-fluorodeoxyglucose (FDG), a proxy for regional cerebral metabolism, and of amyloid deposition from ^{18}F-florbetapir scans were downloaded from the Alzheimer's Disease Neuroimaging Initiative (ADNI) database. Scans from E4 homozygotes were compared to scans from *APOE*E4* non-carriers.

Subjects and Methods

Participants

Data used in the preparation of this article were obtained from the Alzheimer's Disease

Neuroimaging Initiative (ADNI) database (adni.loni.usc.edu; RRID:SCR_003007; accessed 5/2017). The ADNI was launched in 2003 as a public-private partnership, led by Principal Investigator Michael W. Weiner, MD. The primary goal of ADNI has been to test whether serial magnetic resonance imaging (MRI), positron emission tomography (PET), other biological markers, and clinical and neuropsychological assessment can be combined to measure the progression of mild cognitive impairment (MCI) and early Alzheimer's disease (AD).

All E4/E4 subjects (N = 8) included here had no memory complaints or functional impairments and were identified as normal cognitively based on neurological and neuropsychological testing; Mini-Mental Status Exam (MMSE) score 24-30; absence of clinically significant findings on screening MRI; Clinical Dementia Rating (CDR) 0; Geriatric Depression Scale (GDS) ≤ 6; and Hachinski score < 4. This designation was based on the diagnosis closest to the time of the first imaging scan. Imaging results (e.g., cortical thinning, FDG, amyloid) were not used to define normalcy; so, normal volunteers could have abnormalities in imaging scans subsequently. One homozygote did not get an amyloid scan. The comparison group was likewise characterized as normal but lacked E4 carriers. Demographic characteristics and related data of the homozygotes are shown in Table 1.

Additionally, LOAD subjects (N = 8) from ADNI with very mild AD (CDR sum of boxes mean = 3.4; range 2-4.5; SD = 1) and similar ages to E4/E4 group were selected as a patient group for comparison to the observations on asymptomatic homozygotes. As

reviewed in the Discussion, there is already an extensive convergent literature on metabolic changes in AD.

Methods

All methods are described in detail at the ADNI database (adni.loni.usc.edu) following procedures approved by the institutional review boards. All scanning manufacturer's corrections were "On" (decay, randoms, scatter, etc.).

Briefly, subjects were injected intravenously with 185 MBq (5 mCi) ^{18}F-FDG for the glucose-uptake scan. The volunteer rested with eyes and ears open in a quiet, dim room for 20 min. At 30 min after injection, emission scans were obtained for 30 min. Scans were corrected for measured attenuation using low-dose CT scans.

Amyloid scans were acquired within two weeks before or after the FDG scans. The subjects were injected intravenously with 370 MBq (10 mCi) ^{18}F-florbetapir. After a 50-minute uptake period, an emission scan was obtained for 20 min. Scans were corrected for measured attenuation using low-dose CT scans.

Image Analysis

All scans consisted of a 160 x 160 x 96 image grid with a voxel size of 1.5 mm cubic voxels. Scanner specific filters were used to obtain regardless of scanner model an image resolution of approximately 8 mm FWHM. Images were inspected visually for potential artifacts. The FDG PET scans were normalized to a whole-brain uptake of 1000 counts. The amyloid scans were normalized based on the cerebellar cortex. All

scans were anatomically coregistered to a template using Neurostat (Stereotactic Image Registration; Version 7.1; S. Minoshima, University of Utah). Minima and maxima of the Z-images were localized and quantitated with in-house software using an averaged, roving, 3-voxel cube. As routine for FDG PET studies at this resolution, a Z-score ≥ 3.0 was defined as significant. The localization of structures was aided through use of the Talairach daemon (Lancaster et al., 2000).

Results

The demographics and related data of the *APOE*E4* homozygotes are presented in Table 1. The average age was 76 years, range 66-85, SD 8. Three volunteers were women. The average of MMSE scores was 29. SUVR ranged from 0.93 to 1.53 (mean 1.02; SD 0.04); four were classified as amyloid positive by ADNI criteria. Hachinski scores ranged from 0 to 1 with average of 0.5. The average GDS ratings was 1.5. The reference control group (i.e., non-E4 carriers; including E2 and E3 genotypes) was matched for age (75 years, range 60-94, SD 6) and educational level (17 years). The reference group for FDG PET included 282 subjects; 144 males, 138 females; education range 8-20 years, mean = 16.6; 254 Euroamericans, 17 African Americans; 6 Asian Pacific Americans; and 1 Native American. The reference control group for amyloid imaging included 263 subjects; 133 males, 130 females; 235 Euroamericans, 17 African Americans, 6 Asian Pacific Americans; and 1 Native American.

Figure 1 (upper panel) shows the peak regions of hypometabolism based on ^{18}F-FDG when comparing subjects who were *APOE*E4* homozygotes vs. *APOE*E4* non-carriers.

Both medial temporal cortices were symmetrically hypometabolic (left greater than right). The peak of hypometabolism mapped to left parahippocampal gyrus, Brodmann 37, at (-39, -37, -11) with Z = -3.0. Although below the significance threshold, the second most hypometabolic peak localized to the left hippocampus at (-33, -15, -14) with Z = -2.6. No other regions were hypometabolic including the putamen or ACC. No regions showed increased metabolism in the contrast between homozygotes and non-carriers.

Figure 1 (lower panel) shows the results for same metabolism contrast (LOAD vs. non-carrier). There is medial temporal hypometabolism similar in magnitude to that seen in E4/E4. As expected, large foci of hypometabolism localized to the PCC, ACC, lateral parietal and inferior temporal cortices.

Figure 2 (upper panel) shows the loci of peak deposition of amyloid based on ^{18}F-florbetapir in *APOE*E4* homozygotes when compared to the E4 non-carrier group. The peaks with highest magnitude localized to the lenticular nuclei particularly the bilateral putamen. A broad region of amyloid deposition occurred in the ACC as well as medial and middle prefrontal gyri, inferior temporal, and occipital gyri. Other foci are listed in Table 2. No amyloid mapped to the PCC.

Figure 2 (lower panel) shows the results for the same amyloid contrast (LOAD vs. non-carrier). Most of the cortex shows extensive deposition of amyloid. The bilateral putamen show the greatest magnitude of deposition along with very heavy deposits in PCC/precuneus, ACC, as well as prefrontal, lateral parietal, and lateral temporal

cortices. As reviewed below, these results converge with extensive literature but are presented for direct comparison with the homozygotes.

Discussion

Novel findings in E4 homozygotes

This report provides several new findings. The literature relevant to these results based on metabolic and amyloid imaging as well as limitations are presented in the subsequent sections. 1) MTL metabolism was reduced in E4 homozygotes like the results found here in LOAD, albeit the latter had more extensive lateral temporal changes. Nevertheless, reports of MTL metabolism in relation to E4 status have been mixed. Although cognitively-intact E4 homozygotes are widely considered to show similar patterns of hypometabolism to patients with early LOAD, there are also numerous regions where they differ; e.g., E4 homozygotes show more extensive hypometabolism in the prefrontal cortex than do those with early AD. 2) E4 homozygotes did not show the anticipated parietal hypometabolism found by others as reviewed below. Examining all hypometabolic foci, a PCC region occurs at Z = -2.0--far below the significance cutoff, which could be a Type II error given the small sample size. However, similar sample sizes in MCI or AD show robust PCC hypometabolism as seen in LOAD here. The E4 homozygotes in this study were older than in other studies. The absence of parietal hypometabolism could reflect a degree of resilience against AD despite carrying the risk alleles (i.e., sampling bias). 3) E4 homozygotes showed the greatest degree of amyloid deposition in bilateral putamen. Numerous studies as noted below have shown the PCC/precuneus and prefrontal cortices have high amyloid loads

in cognitively normal adults, early onset AD, LOAD, and those carrying AD-relevant mutations. However, mutation carriers show highest amyloid deposition in striatum. 4) The E4 homozygotes showed no hypometabolism in the putamen, the principal site of amyloid deposition. This is consistent with studies of preclinical and clinical carriers of AD-relevant mutations. 5) Extensive accumulation of amyloid in E4 homozygotes localized to several additional regions including the ACC, medial frontal, middle frontal, inferior temporal, middle temporal, superior temporal, and occipital regions.

Hypometabolism in AD, E4 and Autosomal Dominant Carriers

Metabolic changes in AD

FDG PET remains among the best methods to evaluate functional brain decline in cognitively-intact E4 carriers as well as in both preclinical and clinical early onset AD (EOAD) and sporadic LOAD. EOAD is classified typically as onset before 65 years. Many studies of EOAD do not systematically screen to exclude carriers of known mutations. Across studies the greatest consistency and degree of hypometabolism localizes to the PCC/precuneus (see below). It was unanticipated the MTL was not the principal region of hypometabolism given its role in memory, site of tau deposition, and atrophy in normal aging and AD. However, the large partial volume effects and inter-slice distances in early PET scanners likely reduced sensitivity to detection.

Kim et al. (2005) studied 74 EOAD (< 65 years; CDR 0.5) using FDG PET. They reported more severe hypometabolism in parietal, frontal and subcortical (basal ganglia and thalamus) areas when compared to LOAD, interpreted as a more rapid deteriorating course. Rabinovici et al. (2010) reported EOAD (< 65 years) had more

294 severe deficits in working memory and attention. EOAD had more severe PCC and
295 bilateral temporoparietal hypometabolism than LOAD; LOAD did not show relative
296 decreases in metabolism compared to EOAD. EOAD had lower metabolism after
297 atrophy correction than LOAD in bilateral precuneus and right angular gyrus; no regions
298 in LOAD were less metabolic than in EOAD. There was a positive correlation between
299 age of onset and hypometabolism in the precuneus, lateral parietal and occipital
300 regions.

301 The initial region of hypometabolism in early LOAD localized typically to the
302 PCC/precuneus with subsequent extension into biparietal and inferior temporal regions
303 (Minoshima et al., 1994; Minoshima et al., 1997). Despite the noteworthy absence of
304 MTL hypometabolism in early studies, most subsequent studies using FDG PET on
305 higher resolution scanners or with inter-leaf acquisition demonstrated hypometabolism
306 in the MTL along the continuum from normal to MCI to AD; this hypometabolism
307 predicted subsequent cognitive decline (Mosconi et al., 2008; Chen et al., 2010;
308 Lehmann et al., 2014).

309 **Metabolic changes with carriage of E4 allele**

310 Several studies examined alterations in metabolism in presymptomatic subjects and
311 LOAD relative to E4 allele status. Small et al. (1995) compared FDG PET scans from
312 cognitively-intact subjects (age ~55 years) with mild memory complaints both with (N =
313 12) and without (N = 19) the E4 allele. They found E4 carriers had marked
314 hypometabolism in both parietal lobes. Reiman et al. (2001) compared metabolic
315 decline over a two-year interval in cognitively-normal APOE carriers vs. non-carriers

316 (50-63 years). They demonstrated despite the absence of cognitive change during
317 follow-up significantly less metabolism in carriers localized to lateral temporal cortex,
318 PCC, lateral prefrontal cortex, basal forebrain, parahippocampal/lingual gyri, and
319 thalamus. Langbaum et al. (2009) compared FDG PET scans from elder normal control
320 subjects and patients with amnestic MCI and AD. Despite higher resolution (8 mm
321 FWHM) scans, medial temporal hypometabolism was detected bilaterally only in the AD
322 patients compared with control subjects. There was hypometabolism in bilateral
323 precuneus and left lateral parietal lobe in normal subjects with E4 allele as compared to
324 those without E4 (N = 21 and 61 in each group, respectively).

325 In a landmark publication, Reiman et al. (1996) contrasted 1) FDG PET of 11
326 cognitively-intact E4 homozygotes with 22 healthy controls without the E4 allele (mean
327 group age: 55 and 56 years, respectively); and 2) FDG PET of 37 probable AD patients
328 with 22 healthy controls (each group of average age 64 years). The probable AD
329 patients relative to matched controls showed three broad regions of hypometabolism:
330 PCC/precuneus as well as bilateral parietal and bilateral inferior temporal lobes. In
331 addition, there were several small foci of hypometabolism in the prefrontal, occipital and
332 lateral temporal regions. Medial temporal hypometabolism was not reported in the AD
333 patients. In the contrast involving E4 homozygotes vs. those without E4 allele, several
334 hypometabolic foci converged with the AD hypometabolic regions including the
335 PCC/precuneus, parietal, and inferior temporal cortices. Of note, the E4 homozygotes
336 also had broad regions of significant hypometabolism in the prefrontal cortices as well
337 as smaller foci distributed throughout the cortex and cerebellum not seen in the AD
338 group.

In a subsequent study, Reiman et al (2004) examined with FDG PET healthy middle-aged adults (20-39 years). Twelve E4 heterozygotes when compared to 15 E4 no-carriers showed some overlap with hypometabolic regions seen in AD particularly in PCC/precunueus as well as in parietal and inferior temporal regions. Medial temporal changes were not reported. The heterozygotes showed several regions of hypometabolism in prefrontal cortex beyond those seen in AD patients. So, hypometabolism can arise both within and outside AD-affected regions even in much younger healthy subjects.

De Leon et al. (2001) noted in a longitudinal study that those having cognitive decline from normal status at baseline showed lateral temporal lobe hypometabolism dependent on E4 status; the entorhinal cortex did not show this effect. Mosconi et al (2004) compared using FDG PET AD patients with and without the E4 allele. They noted an age-by-genotype interaction in the anterior cingulate and medial frontal cortices. The results were interpreted as indicating an age-dependent aggravation in metabolic decline in AD related to the E4 allele status.

To investigate the effects of ethnicity on the relationship of APOE status to glucose metabolism, cognitively intact, middle-aged (mean ~55 years) Latino Mexican-Americans were studied with FDG PET (Langbaum et al., 2010). The left hippocampus had decreased metabolism in E4 carriers vs. non-carriers (N = 11 and 16 per group, respectively). There was some convergence of medial and lateral parietal hypometabolism in the contrast between E4 carriers vs. non-carriers with the hypometabolism seen in LOAD. However, the E4 carriers showed less hypometabolism in the traditional precuneus/PCC regions with more extensive involvement of the ACC.

In contrast, Protas et al. (2013) examined with defined regions of interest a large series of healthy subjects (mean age ~56 years) who carried either 0, 1, or 2 E4 alleles (N = 76, 42, and 31, respectively). They noted a highly significant difference across groups in PCC metabolism; no diffference in hippocampal metabolism or volume was found. Differences in subject groups, technologies, or analysis methods could account for the divergence in results from those reported here. First, the much smaller sample of homozygotes in the present study compared to that of Portas et al. could explain the failure to detect PCC hypometabolism; even the changes in the MTL reported here were not large, although there was some subthreshold hypometabolism in the contralateral hippocampus. The left hippocampal hypometabolism in normal E4 carriers reported here does converge with the observation of Langbaum et al. (2010). Second, the earlier generation scanner used in the Protas et al. report had an inter-slice distance of 3.375 mm; this slice thickness without three-dimensional acquisition or volume reconstruction would decrease recovery of the thin strip of MTL extending inferiorly from posterior to anterior as seen in Fig. 1 in the present report. Third, the mean age of the homozygotes here was much greater than that in the study of Protas et al. study. Fourth, the present analysis used a voxel-wise approach, while Protas et al. used defined regions of interest. Finally, Protas et al. did not report amyloid deposition or longitudinal outcomes that could impact metabolism across subjects and studies.

Metabolic changes in autosomal dominant mutation carriers

Several studies have examined with FDG PET the metabolic changes in mutation carriers including *APP* dosage effects (trisomy 21/Down's syndrome; *APP* duplication; exon deletion variant) as well as mutations in *PSEN1*, *PSEN2*, and *APP*. Villemagne et

al. (2009) found the classic PCC and biparietal pattern of hypometabolism seen in sporadic AD was not as evident in mutation carriers (N = 8; CDR 0-3.0). No distinct pattern of FDG hypometabolism characterized the various PSEN1 vs. APP mutation carriers; three individuals showed an almost normal pattern of uptake including the striatum, the principal locus of amyloid deposition. There was no relation between the hypometabolic pattern in the cortex or striatum and disease severity, type of mutation, or cognitive status. Schöll et al. (2012) reported on 2 *APParc* mutation carriers showing AD-typical patterns of hypometabolism. Sabbagh et al. (2015) reported in Down's syndrome without dementia (mean ~36 years) mostly hypometabolism and decreased grey matter atrophy in the ACC not PCC. Therefore, considerable variability in metabolism is seen in mutation carriers.

Amyloid deposits in EOAD, LOAD, E4 carriers, and autosomal mutation carriers.

Amyloid deposits in AD

Neuropathologically, non-demented control subjects do not show amyloid deposition or neurofibrillary changes (Braak & Braak, 1991). In contrast, patients with AD not only show extensive fibrillar amyloid, but also an abundance of amyloid deposits that are diffuse without neurofibrillary changes or glial reaction (Braak and Braak, 1991; Brilliant et al., 1997). The striatum develops senile neuritic plaques and neurofibrillary tangles later in the progression of AD (Braak stage V-VI; Braak & Braak, 1991).

Amyloid imaging labels fibrillar amyloid (Ikomonovic et al., 2008; Clark et al., 2011; Curtis et al., 2015). Other forms of amyloid (diffuse, fleecy, deposits in AD cerebellum; amyloid oligomers) are not detected. In AD, the greatest fibrillar amyloid deposition

407 localizes to the parietal cortex (both preceuneus/PCC and lateral parietal); parietal
408 fibrillar amyloid deposition often shows a correlation with declining parietal metabolism
409 and synaptic markers (Klunk et al., 2004; Li et al., 2008; Scheff et al., 2015).
410 Subsequently, fibrillar amyloid deposits spread throughout the neocortex including ACC,
411 lateral prefrontal cortex, striatum, and the temporal lobe. Differences in amyloid
412 deposition between EOAD compared to LOAD have depended on the region of interest.
413 Rabinovici et al. (2010) studied 18 EOAD and compared them to 16 LOAD. They found
414 no effect on amyloid deposition but decreasing metabolism in posterior brain regions
415 depending on age of onset. Youn et al. (2017) studied nine EOAD, 11 LOAD, and eight
416 normal controls. EOAD patients were screened negative for the common AD-associated
417 mutations. EOAD patients showed greater amyloid deposition only in the thalamus and
418 basal ganglia compared to those with LOAD.

419 **Amyloid deposits and *APOE*E4***

420 The major locus of amyloid deposition found here in E4 homozygotes localized to the
421 putamen as well as several other regions (ACC, medial frontal, middle frontal, inferior
422 temporal, middle temporal, superior temporal, and occipital). Unlike what is seen in
423 typical LOAD, neither hypometabolism nor amyloid deposition localized to the PCC in
424 these E4 homozygotes. It is noteworthy that the localization of fibrillar amyloid in healthy
425 elders and in AD does not reflect the patterns of cortical thinning, hypometabolism, or
426 clinical phenotypes; these appear to converge with the localization of tau
427 (Ossenkoppele et al., 2016; Schöll et al., 2016; Xia et al., 2017; Lockhart et al., 2017;
428 Pontecorvo et al., 2017)

The pattern of amyloid deposition noted here is not inconsistent with that reported by Reiman et al. (2009). They studied a younger group (mean age ~63 years) of eight homozygotes, 12 heterozygotes, and 12 non-carriers of E4. They reported a significant association with "AD-affected mean cortical, frontal, temporal, posterior cingulate-precuneus, parietal, and basal ganglia ROIs…" Based on an estimation of the basal ganglia data (Fig. 1), reanalysis specifically comparing E4 homozygotes to non-carriers, analogous to that done here, produced $p < 0.01$ (two-tailed, between sample t-test; df = 18; heteroscedastic correction) indicating convergence in findings. Given the older age of the current homozygotes, amyloid deposition here appeared grossly greater overall than that reported by Reiman et al. (2009).

Amyloid deposits in autosomal dominant mutations

Genetic familial effects beyond those associated with the E4 allele have been reported with APP gene dose (trisomy 21/Down's syndrome; APP duplication) as well as mutations in PSEN1, PSEN2, and APP. Putaminal amyloid deposits, which can correlate with age early in the course, were seen in Down's syndrome without dementia (Handen et al., 2012; Lao et al., 2016). Braak stage (based on tau scans), amyloid deposition, and cognitive decline were correlated with age in amyloid-positive, non-demented subjects with Down's syndrome; glucose hypometabolism and tau did not localize to the striatum, although regions with hypometabolism overlapped areas with tau deposition (Rafii et al., 2017). High levels of amyloid in the putamen were reported also in various cases of preclinical and clinical AD related to PSEN1, PSEN2, and APP mutations (Klunk et al., 2007; Remes et al., 2008; Koivunen et al., 2008; Villemagne et

al., 2009; Fleisher et al., 2012; Shi et al., 2015; Rodriguez-Vieitez et al., 2016). Like observations here about E4 homozygotes, AD mutation carriers with putaminal amyloid deposits did not show hypometabolism in the putamen (Rodriguez-Vieitez et al., 2016).

The clinical significance of striatal amyloid deposition is unclear. The co-occurrence of Parkinson's in AD is well known. AD variants with mutations such as APP can also have various motor manifestations such as hyperactive reflexes, extremity weakness, and spastic paraparesis. An increased incidence of Parkinson's in subjects with Down's syndrome with or without dementia remains controversial (Hestnes et al., 1997).

Limitations

The major limitation of this study is the small number of homozygotes available in the ADNI database, not surprising given their low frequency. The ALZGENE database indicates an E4/E4 prevalence of approximately 2% in controls and 15% in AD cases (Alzforum, 2017). Furthermore, the frequency of E4/E4 decreases with aging most likely related to differential survival related to cardiovascular disease. In an Australian community sample of those 70 years of age or older surviving a follow-up period of 3 years, the E4 allele frequency was 13% (Henderson et al., 1995). Of these 638 subjects, only ten E4 homozygotes were recruited, and none were older than 90 years. Larger samples will require pooling across multiple databases. The limited sample described here risks Type II errors; so, the present findings must be considered preliminary particularly regarding the absence of changes in various regions. Nevertheless, the present findings are noteworthy given the differences from LOAD and similarities to AD-related mutations and Down's syndrome.

Another issue concerns whether the homozygotes represent typical preclinical AD or whether the sample is biased (e.g., survival bias). Despite normal cognitive status, approximately half were already positive for amyloid by the usual criteria (ADNI's templated SUVR). Their mean age of approximately 76 years is near the peak age (60-75 years) for the highest risk of conversion from normal cognition to MCI or AD (Bonham et al., 2016). The predicted age for onset of LOAD in E4 homozygotes has been estimated at 5-7 years earlier than for non-carriers (Blacker et al., 1997; Sando et al., 2008).

No atrophy correction was made for the measurements of glucose metabolism in this study. The between-group comparison minimized age-related atrophy across groups by matching on age. The rationale for not performing atrophy correction considered that depending on the algorithm, amplification of noise compounded by the small sample size can introduce additional concerns. The question of PCC and medial temporal atrophy in cognitively-normal E4 carriers is controversial given mixed results from different studies. For example, Li et al. (2016) found greater atrophy of the left hippocampus in E4 carrier vs. noncarrier groups without dementia (i.e., control and MCI cobmined) from ADNI (N = 212 and 242 per group, respectively). Haller et al. (2017) studied adults (N = 282) dwelling in the community who were cognitively intact and followed for 18 months. They found a significant effect of the E4 allele on PCC atrophy but only for those who decline on follow-up; no changes were found in the MTL. The MTL in elderly with intact cognition is known to have tau tangles typically associated with neurodegeneration, whether amyloid positive or negative, and may explain the

observed hypometabolism found in this study (Bouras et al., 1994; Braak and Del Tredici, 2015).

Summary

In conclusion, cognitively normal, elderly E4/E4 show an atypical pattern of both hypometabolism and amyloid deposition compared to that known to occur in LOAD. Metabolism is dissociated in localization from amyloid deposition. The region of greatest amyloid deposition localizes to the putamen as is seen in Down's syndrome and early onset AD arising from mutations. The mechanisms for protein deposition remain unclear. The difference in biomarker phenotypes between E4 homozygotes and those with LOAD suggest either divergent pathophysiological processes, unshared environmental effects, or residuals of resilience to AD in a high risk group.

References Cited

Alzforum (2017) Alzgene - meta-analysis of all published AD association studies (case-control only) APOE e2/3/4 In: Biomedical Research Forum.

Blacker D, Haines JL, Rodes L, Terwedow H, Go RC, Harrell LE, Perry RT, Bassett SS, Chase G, Meyers D, Albert MS, Tanzi R (1997) APOE-4 and age at onset of Alzheimer's disease: the NIMH genetics initiative. Neurology 48:139-147.

Bonham LW, Geier EG, Fan CC, Leong JK, Besser L, Kukull WA, Kornak J, Andreassen OA, Schellenberg GD, Rosen HJ, Dillon WP, Hess CP, Miller BL, Dale AM, Desikan RS, Yokoyama JS (2016) Age-dependent effects of APOE epsilon4 in preclinical Alzheimer's disease. Ann Clin Transl Neurol 3:668-677.

Bouras C, Hof PR, Giannakopoulos P, Michel JP, Morrison JH (1994) Regional distribution of neurofibrillary tangles and senile plaques in the cerebral cortex of elderly patients: a quantitative evaluation of a one-year autopsy population from a geriatric hospital. Cereb Cortex 4:138-150.

Braak H, Braak E (1991) Neuropathological staging of Alzheimer-related changes. Acta Neuropathol 82:239-259.

Braak H, Del Tredici K (2015) The preclinical phase of the pathological process underlying sporadic Alzheimer's disease. Brain 138:2814-2833.

Brilliant MJ, Elble RJ, Ghobrial M, Struble RG (1997) The distribution of amyloid beta protein deposition in the corpus striatum of patients with Alzheimer's disease. Neuropathol Appl Neurobiol 23:322-325.

527 Chen K, Langbaum JB, Fleisher AS, Ayutyanont N, Reschke C, Lee W, Liu X, Bandy D,
528 Alexander GE, Thompson PM, Foster NL, Harvey DJ, de Leon MJ, Koeppe RA, Jagust
529 WJ, Weiner MW, Reiman EM, Alzheimer's Disease Neuroimaging I (2010) Twelve-
530 month metabolic declines in probable Alzheimer's disease and amnestic mild cognitive
531 impairment assessed using an empirically pre-defined statistical region-of-interest:
532 Findings from the Alzheimer's disease neuroimaging initiative. Neuroimage 51:654-664.

533 Clark CM et al. (2011) Use of florbetapir-PET for imaging beta-amyloid pathology.
534 JAMA 305:275-283.

535 Curtis C et al. (2015) Phase 3 trial of flutemetamol labeled with radioactive fluorine 18
536 imaging and neuritic plaque density. JAMA Neurology 72:287-294.

537 de Leon MJ, Convit A, Wolf OT, Tarshish CY, DeSanti S, Rusinek H, Tsui W, Kandil E,
538 Scherer AJ, Roche A, Imossi A, Thorn E, Bobinski M, Caraos C, Lesbre P, Schlyer D,
539 Poirier J, Reisberg B, Fowler J (2001) Prediction of cognitive decline in normal elderly
540 subjects with 2-[(18)F]fluoro-2-deoxy-d-glucose/positron-emission tomography
541 (FDG/PET). Proc Natl Acad Sci U S A 98:10966-10971.

542 Donohue MC, Sperling RA, Petersen R, Sun CK, Weiner MW, Aisen PS, Alzheimer's
543 Disease Neuroimaging I (2017) Association between elevated brain amyloid and
544 subsequent cognitive decline among cognitively normal persons. JAMA 317:2305-2316.

545 Doraiswamy PM, Sperling RA, Johnson K, Reiman EM, Wong TZ, Sabbagh MN,
546 Sadowsky CH, Fleisher AS, Carpenter A, Joshi AD, Lu M, Grundman M, Mintun MA,
547 Skovronsky DM, Pontecorvo MJ, Group AAS, Group AAS (2014) Florbetapir F-18

548 amyloid PET and 36-month cognitive decline: a prospective multicenter study. Mol
549 Psychiatry 19:1044-1051.

550 Farrer LA, Cupples LA, Haines JL, Hyman B, Kukull WA, Mayeux R, Myers RH,
551 Pericak-Vance MA, Risch N, van Duijn CM (1997) Effects of age, sex, and ethnicity on
552 the association between apolipoprotein E genotype and Alzheimer disease. A meta-
553 analysis. APOE and Alzheimer Disease Meta-analysis Consortium. JAMA 278:1349-
554 1356.

555 Fleisher AS et al., (2012) Florbetapir PET analysis of amyloid-beta deposition in the
556 presenilin 1 E280A autosomal dominant Alzheimer's disease kindred: a cross-sectional
557 study. Lancet Neurol 11:1057-1065.

558 Genin E et al., (2011) APOE and Alzheimer disease: a major gene with semi-dominant
559 inheritance. Mol Psychiatry 16:903-907.

560 Haller S, Montandon ML, Rodriguez C, Ackermann M, Herrmann FR, Giannakopoulos P
561 (2017) APOE*E4 is associated with gray matter loss in the posterior cingulate cortex in
562 healthy elderly controls subsequently developing subtle cognitive decline. AJNR Am J
563 Neuroradiol 38:1335-1342.

564 Handen BL, Cohen AD, Channamalappa U, Bulova P, Cannon SA, Cohen WI, Mathis
565 CA, Price JC, Klunk WE (2012) Imaging brain amyloid in nondemented young adults
566 with Down syndrome using Pittsburgh Compound B. Alzheimers Dement 8:496-501.

567 Henderson AS, Easteal S, Jorm AF, Mackinnon AJ, Korten AE, Christensen H, Croft L,
568 Jacomb PA (1995) Apolipoprotein E allele epsilon 4, dementia, and cognitive decline in
569 a population sample. Lancet 346:1387-1390.

570 Hestnes A, Daniel SE, Lees AJ, Brun A (1997) Down's syndrome and Parkinson's
571 disease. J Neurol Neurosurg Psychiatry 62:289.

572 Ikonomovic MD, Klunk WE, Abrahamson EE, Mathis CA, Price JC, Tsopelas ND,
573 Lopresti BJ, Ziolko S, Bi W, Paljug WR, Debnath ML, Hope CE, Isanski BA, Hamilton
574 RL, DeKosky ST (2008) Post-mortem correlates of in vivo PIB-PET amyloid imaging in
575 a typical case of Alzheimer's disease. Brain 131:1630-1645.

576 Kim EJ, Cho SS, Jeong Y, Park KC, Kang SJ, Kang E, Kim SE, Lee KH, Na DL (2005)
577 Glucose metabolism in early onset versus late onset Alzheimer's disease: An SPM
578 analysis of 120 patients. Brain 128:1790-1801.

579 Klunk WE et al., (2004) Imaging brain amyloid in Alzheimer's disease with Pittsburgh
580 Compound-B. Ann Neurol 55:306-319.

581 Klunk WE et al., (2007) Amyloid deposition begins in the striatum of presenilin-1
582 mutation carriers from two unrelated pedigrees. J Neurosci 27:6174-6184.

583 Koivunen J, Verkkoniemi A, Aalto S, Paetau A, Ahonen JP, Viitanen M, Någren K,
584 Rokka J, Haaparanta M, Kalimo H, Rinne JO (2008) PET amyloid ligand [(11)C]PIB
585 uptake shows predominantly striatal increase in variant Alzheimer's disease. Brain
586 131:1845-1853.

587 Lancaster JL, Woldorff MG, Parsons LM, Liotti M, Freitas CS, Rainey L, Kochunov PV,
588 Nickerson D, Mikiten SA, Fox PT (2000) Automated Talairach atlas labels for functional
589 brain mapping. Hum Brain Mapp 10:120-131.

590 Langbaum JB, Chen K, Lee W, Reschke C, Bandy D, Fleisher AS, Alexander GE,
591 Foster NL, Weiner MW, Koeppe RA, Jagust WJ, Reiman EM (2009) Categorical and
592 correlational analyses of baseline fluorodeoxyglucose positron emission tomography
593 images from the Alzheimer's Disease Neuroimaging Initiative (ADNI). Neuroimage
594 45:1107-1116.

595 Langbaum JB, Chen K, Caselli RJ, Lee W, Reschke C, Bandy D, Alexander GE, Burns
596 CM, Kaszniak AW, Reeder SA, Corneveaux JJ, Allen AN, Pruzin J, Huentelman MJ,
597 Fleisher AS, Reiman EM (2010) Hypometabolism in Alzheimer-affected brain regions in
598 cognitively healthy Latino individuals carrying the apolipoprotein E epsilon4 allele. Arch
599 Neurol 67:462-468.

600 Lao PJ, Betthauser TJ, Hillmer AT, Price JC, Klunk WE, Mihaila I, Higgins AT, Bulova
601 PD, Hartley SL, Hardison R, Tumuluru RV, Murali D, Mathis CA, Cohen AD, Barnhart
602 TE, Devenny DA, Mailick MR, Johnson SC, Handen BL, Christian BT (2016) The effects
603 of normal aging on amyloid-beta deposition in nondemented adults with Down
604 syndrome as imaged by carbon 11-labeled Pittsburgh Compound B. Alzheimers
605 Dement 12:380-390.

606 Lehmann M, Ghosh PM, Madison C, Karydas A, Coppola G, O'Neil JP, Huang Y, Miller
607 BL, Jagust WJ, Rabinovici GD (2014) Greater medial temporal hypometabolism and

608 lower cortical amyloid burden in APOE4-positive AD patients. J Neurol Neurosurg
609 Psychiatry 85:266-273

610 Li B, Shi J, Gutman BA, Baxter LC, Thompson PM, Caselli RJ, Wang Y, Alzheimer's
611 Disease Neuroimaging I (2016) Influence of APOE genotype on hippocampal atrophy
612 over time - an n = 1925 surface-based ADNI study. PLoS One 11:e0152901.

613 Li Y, Rinne JO, Mosconi L, Pirraglia E, Rusinek H, DeSanti S, Kemppainen N, Någren
614 K, Kim BC, Tsui W, de Leon MJ (2008) Regional analysis of FDG and PIB-PET images
615 in normal aging, mild cognitive impairment, and Alzheimer's disease. Eur J Nucl Med
616 Mol Imaging 35:2169-2181.

617 Lockhart SN, Schöll M, Baker SL, Ayakta N, Swinnerton KN, Bell RK, Mellinger TJ,
618 Shah VD, O'Neil JP, Janabi M, Jagust WJ (2017) Amyloid and tau PET demonstrate
619 region-specific associations in normal older people. Neuroimage 150:191-199.

620 Minoshima S, Foster NL, Kuhl DE (1994) Posterior cingulate cortex in Alzheimer's
621 disease. Lancet 344:895.

622 Minoshima S, Giordani B, Berent S, Frey KA, Foster NL, Kuhl DE (1997) Metabolic
623 reduction in the posterior cingulate cortex in very early Alzheimer's disease. Ann Neurol
624 42:85-94.

625 Monsell SE, Kukull WA, Roher AE, Maarouf CL, Serrano G, Beach TG, Caselli RJ,
626 Montine TJ, Reiman EM (2015) Characterizing apolipoprotein E epsilon4 carriers and
627 noncarriers with the clinical diagnosis of mild to moderate Alzheimer dementia and
628 minimal beta-amyloid peptide plaques. JAMA neurology 72:1124-1131.

629 Morris JC, Roe CM, Xiong C, Fagan AM, Goate AM, Holtzman DM, Mintun MA (2010)
630 APOE predicts amyloid-beta but not tau Alzheimer pathology in cognitively normal
631 aging. Ann Neurol 67:122-131.

632 Mosconi L, De Santi S, Li J, Tsui WH, Li Y, Boppana M, Laska E, Rusinek H, de Leon
633 MJ (2008) Hippocampal hypometabolism predicts cognitive decline from normal aging.
634 Neurobiol Aging 29:676-692.

635 Mosconi L, Sorbi S, Nacmias B, De Cristofaro MT, Fayyaz M, Bracco L, Herholz K, Pupi
636 A (2004) Age and APOE genotype interaction in Alzheimer's disease: An FDG-PET
637 study. Psychiatry Res 130:141-151.

638 Murray J, Tsui WH, Li Y, McHugh P, Williams S, Cummings M, Pirraglia E, Solnes L,
639 Osorio R, Glodzik L, Vallabhajosula S, Drzezga A, Minoshima S, de Leon MJ, Mosconi
640 L (2014) FDG and amyloid PET in cognitively normal individuals at risk for late-onset
641 Alzheimer's disease. Adv J Mol Imaging 4:15-26.

642 Ossenkoppele R, Schonhaut DR, Schöll M, Lockhart SN, Ayakta N, Baker SL, O'Neil
643 JP, Janabi M, Lazaris A, Cantwell A, Vogel J, Santos M, Miller ZA, Bettcher BM, Vossel
644 KA, Kramer JH, Gorno-Tempini ML, Miller BL, Jagust WJ, Rabinovici GD (2016) Tau
645 PET patterns mirror clinical and neuroanatomical variability in Alzheimer's disease.
646 Brain 139:1551-1567.

647 Pontecorvo MJ, Devous MD, Sr., Navitsky M, Lu M, Salloway S, Schaerf FW, Jennings
648 D, Arora AK, McGeehan A, Lim NC, Xiong H, Joshi AD, Siderowf A, Mintun MA,

649 investigators FA-A (2017) Relationships between flortaucipir PET tau binding and
650 amyloid burden, clinical diagnosis, age and cognition. Brain 140:748-763.

651 Protas HD, Chen K, Langbaum JB, Fleisher AS, Alexander GE, Lee W, Bandy D, de
652 Leon MJ, Mosconi L, Buckley S, Truran-Sacrey D, Schuff N, Weiner MW, Caselli RJ,
653 Reiman EM (2013) Posterior cingulate glucose metabolism, hippocampal glucose
654 metabolism, and hippocampal volume in cognitively normal, late-middle-aged persons
655 at 3 levels of genetic risk for Alzheimer disease. JAMA neurology 70:320-325.

656 Rabinovici GD, Furst AJ, Alkalay A, Racine CA, O'Neil JP, Janabi M, Baker SL, Agarwal
657 N, Bonasera SJ, Mormino EC, Weiner MW, Gorno-Tempini ML, Rosen HJ, Miller BL,
658 Jagust WJ (2010) Increased metabolic vulnerability in early-onset Alzheimer's disease
659 is not related to amyloid burden. Brain 133:512-528.

660 Rafii MS, Lukic AS, Andrews RD, Brewer J, Rissman RA, Strother SC, Wernick MN,
661 Pennington C, Mobley WC, Ness S, Matthews DC, Down Syndrome Biomarker I, the
662 Alzheimer's Disease Neuroimaging I (2017) PET imaging of tau pathology and
663 relationship to amyloid, longitudinal MRI, and cognitive change in Down syndrome:
664 results from the Down Syndrome Biomarker Initiative (DSBI). J Alzheimers Dis 60:439-
665 450.

666 Reiman EM, Caselli RJ, Yun LS, Chen K, Bandy D, Minoshima S, Thibodeau SN,
667 Osborne D (1996) Preclinical evidence of Alzheimer's disease in persons homozygous
668 for the epsilon 4 allele for apolipoprotein E. N Engl J Med 334:752-758

669 Reiman EM, Caselli RJ, Chen K, Alexander GE, Bandy D, Frost J (2001) Declining
670 brain activity in cognitively normal apolipoprotein E epsilon 4 heterozygotes: A
671 foundation for using positron emission tomography to efficiently test treatments to
672 prevent Alzheimer's disease. Proc Natl Acad Sci U S A 98:3334-3339.

673 Reiman EM, Chen K, Alexander GE, Caselli RJ, Bandy D, Osborne D, Saunders AM,
674 Hardy J (2004) Functional brain abnormalities in young adults at genetic risk for late-
675 onset Alzheimer's dementia. Proc Natl Acad Sci U S A 101:284-289.

676 Reiman EM, Chen K, Liu X, Bandy D, Yu M, Lee W, Ayutyanont N, Keppler J, Reeder
677 SA, Langbaum JB, Alexander GE, Klunk WE, Mathis CA, Price JC, Aizenstein HJ,
678 DeKosky ST, Caselli RJ (2009) Fibrillar amyloid-beta burden in cognitively normal
679 people at 3 levels of genetic risk for Alzheimer's disease. Proc Natl Acad Sci U S A
680 106:6820-6825.

681 Remes AM, Laru L, Tuominen H, Aalto S, Kemppainen N, Mononen H, Någren K,
682 Parkkola R, Rinne JO (2008) Carbon 11-labeled Pittsburgh Compound B positron
683 emission tomographic amyloid imaging in patients with APP locus duplication. Arch
684 Neurol 65:540-544.

685 Rodriguez-Vieitez E, Saint-Aubert L, Carter SF, Almkvist O, Farid K, Schöll M, Chiotis
686 K, Thordardottir S, Graff C, Wall A, Langstrom B, Nordberg A (2016) Diverging
687 longitudinal changes in astrocytosis and amyloid PET in autosomal dominant
688 Alzheimer's disease. Brain 139:922-936.

689 Sabbagh MN, Chen K, Rogers J, Fleisher AS, Liebsack C, Bandy D, Belden C, Protas
690 H, Thiyyagura P, Liu X, Roontiva A, Luo J, Jacobson S, Malek-Ahmadi M, Powell J,
691 Reiman EM (2015) Florbetapir PET, FDG PET, AND MRI in Down syndrome individuals
692 with and without Alzheimer's dementia. Alzheimers Dement 11:994-1004.

693 Sando SB, Melquist S, Cannon A, Hutton ML, Sletvold O, Saltvedt I, White LR,
694 Lydersen S, Aasly JO (2008) APOE epsilon 4 lowers age at onset and is a high risk
695 factor for Alzheimer's disease; a case control study from central Norway. BMC Neurol
696 8:9.

697 Scheff SW, Price DA, Ansari MA, Roberts KN, Schmitt FA, Ikonomovic MD, Mufson EJ
698 (2015) Synaptic change in the posterior cingulate gyrus in the progression of
699 Alzheimer's disease. J Alzheimers Dis 43:1073-1090.

700 Schöll M, Lockhart SN, Schonhaut DR, O'Neil JP, Janabi M, Ossenkoppele R, Baker
701 SL, Vogel JW, Faria J, Schwimmer HD, Rabinovici GD, Jagust WJ (2016) PET imaging
702 of tau deposition in the aging human brain. Neuron 89:971-982.

703 Schöll M, Wall A, Thordardottir S, Ferreira D, Bogdanovic N, Langstrom B, Almkvist O,
704 Graff C, Nordberg A (2012) Low PIB PET retention in presence of pathologic CSF
705 biomarkers in Arctic *APP* mutation carriers. Neurology 79:229-236.

706 Shi Y et al. (2017) Apoe4 markedly exacerbates tau-mediated neurodegeneration in a
707 mouse model of tauopathy. Nature 549:523-527.

708 Shi Z, Wang Y, Liu S, Liu M, Liu S, Zhou Y, Wang J, Cai L, Huo YR, Gao S, Ji Y (2015)
709 Clinical and neuroimaging characterization of Chinese dementia patients with PSEN1
710 and PSEN2 mutations. Dement Geriatr Cogn Disord 39:32-40.

711 Small GW, Mazziotta JC, Collins MT, Baxter LR, Phelps ME, Mandelkern MA, Kaplan A,
712 La Rue A, Adamson CF, Chang L, et al. (1995) Apolipoprotein E type 4 allele and
713 cerebral glucose metabolism in relatives at risk for familial Alzheimer disease. JAMA
714 273:942-947.

715 Talairach J, Tournoux (1988) Coplanar Stereotaxic Atlas of the Human Brain. New
716 York: Thieme.

717 Villemagne VL, Ataka S, Mizuno T, Brooks WS, Wada Y, Kondo M, Jones G, Watanabe
718 Y, Mulligan R, Nakagawa M, Miki T, Shimada H, O'Keefe GJ, Masters CL, Mori H,
719 Rowe CC (2009) High striatal amyloid beta-peptide deposition across different
720 autosomal Alzheimer disease mutation types. Arch Neurol 66:1537-1544.

721 Xia C, Makaretz SJ, Caso C, McGinnis S, Gomperts SN, Sepulcre J, Gomez-Isla T,
722 Hyman BT, Schultz A, Vasdev N, Johnson KA, Dickerson BC (2017) Association of in
723 vivo [(18)F]AV-1451 tau PET imaging results with cortical atrophy and symptoms in
724 typical and atypical Alzheimer disease. JAMA neurology 74:427-436.

725 Youn YC, Jang JW, Han SH, Kim H, Seok JW, Byun JS, Park KY, An SSA, Chun IK,
726 Kim S (2017) [(11)C]-PIB PET imaging reveals that amyloid deposition in cases with
727 early-onset Alzheimer's disease in the absence of known mutations retains higher levels
728 of PIB in the basal ganglia. Clin Interv Aging 12:1041-1048.

Table 1. Subject demographics and related data.

FDG ID #	AV45 ID #	Age	Sex	MMSE	Hach	GDS	SUVR	Months	Dx
009_S_4388	009_S_4388	67	M	29	1	2	0.97	0.9	MCI
013_S_4580	013_S_4580	70	F	30	1	2	1.03	24	Nl
014_S_0520	NA	82	F	30	0	1		8.8	MCI
014_S_4577	014_S_4577	85	M	29	1	0	1.17*	-0.8	MCI
027_S_5083	027_S_5083	74	M	28	0	1	1.05	24	Nl
032_S_4348	032_S_4348	66	F	30	0	5	1.42*	7.2	Nl
033_S_4179	033_S_4179	83	M	30	1	1	1.53*	52	Nl
082_S_4339	082_S_4339	84	M	29	1	0	1.41*	25	Nl

Reference group matched for age (mean 75 years, range 60-94, SD 6) and education (mean 17 years: range 8-20).

Abbreviations: AV45, florbetapir; MMSE, Mini-Mental Status Exam Score; Hach, Hachinski Score; GDS, Geriatric Dementia Scale; SUVR, Standardized uptake value ratio (per ADNI); *, denotes amyloid positive (per ADNI); NA, scan not available/done; Nl, normal; MCI, Mild Cognitive Impairment; Dx, last recorded diagnosis. Months denote time interval between closest assessment and FDG PET (+, months to last diagnosis of normal after imaging; - , months to last diagnosis of normal before imaging).

740 **Table 2. Amyloid deposits in cognitively normal E4 homozygotes contrasted with**

741 **E4 non-carriers.**

Structure	Peak Location*			Z-score
	x	y	z	
Putamen	15	12	0	4.7
Inferior occipital BA 18	-35	-85	-5	4.6
Putamen	-15	12	-2	4.5
Middle occipital BA 19	-44	-73	-9	4.2
Inferior temporal BA 20	55	-37	-18	4.1
ACC BA 32	-6	21	36	4.0
ACC BA 32	-8	23	45	4.0
Middle frontal BA 8	28	26	47	4.0
Brodmann area 9	28	41	29	3.9
Inferior temporal BA 20	39	-24	-23	3.8
Middle frontal BA 10	42	50	0	3.7
Medial frontal BA 9	-10	44	20	3.6
Middle frontal BA 8	-24	35	43	3.6
Brodmann area 9	-28	46	27	3.5
Brodmann area 36	-48	-40	-20	3.4
Brodmann area 6	-24	8	56	3.3
Inferior temporal BA 20	-46	-10	-27	3.3
Inferior temporal BA 20	-48	-17	-25	3.2
Brodmann area 10	-10	35	-13	3.2

Superior temporal BA 22	53	1	-2	3.2
Inferior temporal BA 20	35	-1	-34	3.1
Premotor BA 6	28	-13	58	3.1
Middle temporal BA 21	62	-19	-7	3.1

742

743 BA, Brodmann area; ACC, anterior cingulate cortex; Locations in Talairach (Talairach

744 and Tournoux, 1988) coordinates (mm): +x, right; -x, left; +y, anterior; +z, superior.

745

Figure 1. Upper panel (above color bar): FDG uptake in E4 homozygotes contrasted with E4 non-carrier reference group. Transverse sections (upper left inset) are taken from left to right at z = -11, -18, and -25 mm below the inter-commissural plane, respectively. The peak (red; Z = -3.0) is in the left parahippocampus. Note sequential inferiorly directed medial temporal lobe structures. Larger sections from lower left to upper right: z = -2, y = +12, y = -60, x = -10, respectively. Note minimal hypometabolism throughout including striatum. For illustrative purposes, the threshold was set to Z = -3. Note minimal or no hypoactivity in PCC and parietal cortex in E4 homozygotes. **Lower panel: FDG uptake in very mild AD contrasted with E4 non-carrier reference group.** Transverse sections (upper left inset) are taken from left to right at z = -11, -18, and -25 mm below the inter-commissural plane, respectively. Note sequential inferiorly directed medial temporal lobe structures. Larger sections from lower left to upper right: z = -2, y = +12, y = -60, x = -10, respectively. For illustrative purposes, the threshold was set to Z = -3. Note marked hypometabolism in bilateral lateral parietal cortex and PCC/precuneus (dashed circle). Left side of brain is on right side of image (radiological convention).

762

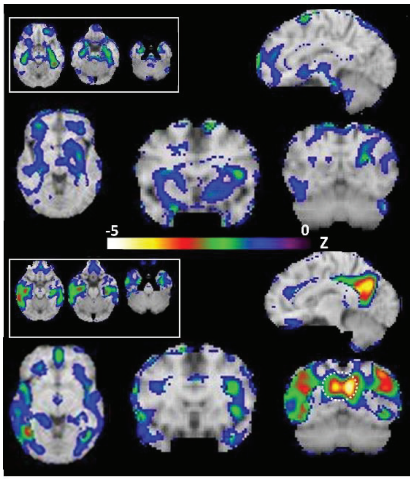

Figure 2. Upper panel (above color bar): Amyloid deposition in cognitively normal, E4 homozygotes contrasted with E4 non-carriers. Transverse sections through MTL (upper left inset) are from left to right at Z = -11, -18, -25, respectively. Larger sections from lower left to upper right: z = -2, y = +12, y = -60, x = -10, respectively. Note heavy amyloid deposition in the striatum, specifically the putamen. The PCC/precuneus (dashed circle) appear to have minimal amyloid unlike the typical pattern in LOAD (see lower panel). For illustrative purposes, the threshold was set to Z = -3. **Lower panel: Amyloid deposition in very mild AD contrasted with E4 non-carriers.** Transverse sections through MTL (upper left inset) are from left to right at Z = -11, -18, -25, respectively. Larger sections from lower left to upper right: z = -2, y = +12, y = -60, x = -10, respectively. Note extensive amyloid deposits throughout the cortex, especially PCC/precuneus, and the striatum. Left side of brain is on right side of image (radiological convention); color bar indicates Z-scores.

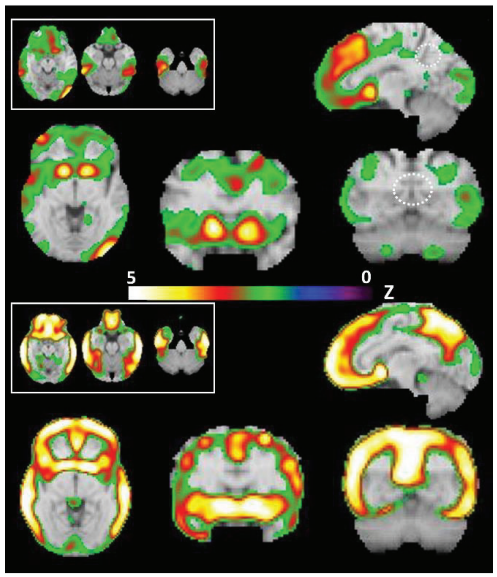

777